

Effect of Dimensionality on the Continuum Percolation of Overlapping Hyperspheres and Hypercubes: II. Simulation Results and Analyses

S. Torquato*

Department of Chemistry, Department of Physics,
Princeton Center for Theoretical Science,
Princeton Institute for the Science and Technology of Materials,
and Program in Applied and Computational Mathematics,
Princeton University, *Princeton NJ 08544*

Y. Jiao[†]

Princeton Institute for the Science and Technology of Materials,
Princeton University, *Princeton NJ 08544*

Abstract

In the first paper of this series [S. Torquato, J. Chem. Phys. **136**, 054106 (2012)], analytical results concerning the continuum percolation of overlapping hyperparticles in d -dimensional Euclidean space \mathbb{R}^d were obtained, including lower bounds on the percolation threshold. In the present investigation, we provide additional analytical results for certain cluster statistics, such as the concentration of k -mers and related quantities, and obtain an upper bound on the percolation threshold η_c . We utilize the tightest lower bound obtained in the first paper to formulate an efficient simulation method, called the *rescaled-particle* algorithm, to estimate continuum percolation properties across many space dimensions with heretofore unattained accuracy. This simulation procedure is applied to compute the threshold η_c and associated mean number of overlaps per particle \mathcal{N}_c for both overlapping hyperspheres and oriented hypercubes for $3 \leq d \leq 11$. These simulations results are compared to corresponding upper and lower bounds on these percolation properties. We find that the bounds converge to one another as the space dimension increases, but the lower bound provides an excellent estimate of η_c and \mathcal{N}_c , even for relatively low dimensions. We confirm a prediction of the first paper in this series that low-dimensional percolation properties encode high-dimensional information. We also show that the concentration of monomers dominate over concentration values for higher-order clusters (dimers, trimers, etc.) as the space dimension becomes large. Finally, we provide accurate analytical estimates of the pair connectedness function and blocking function at their contact values for any d as a function of density.

I. INTRODUCTION

In the first paper (paper I)¹ of this series of two papers, we obtained a number of analytical results concerning the continuum percolation of overlapping hyperspheres and overlapping oriented hypercubes that applied across all Euclidean space dimensions. Among other results, it was shown analytically that certain lower-order Padé approximants on the mean cluster number S are lower bounds on S for both hyperspheres and hypercubes in d -dimensional Euclidean space \mathbb{R}^d and that they become exact asymptotically as $d \rightarrow \infty$. In this asymptotic limit, the dimensionless density at percolation η_c tends to 2^{-d} . An important consequence of the aforementioned analysis is that this large- d percolation value is an important contribution to the low-dimensional percolation value. In other words, low-dimensional results encode high-dimensional information. Percus-Yevick-like approximations for the cluster number S were also obtained that also become asymptotically exact as $d \rightarrow \infty$. The analysis was aided by a striking *duality* between the equilibrium hard-hypersphere (hypercube) fluid system and the continuum percolation models of overlapping hyperspheres (hypercubes), namely,

$$P(r; \eta) = -h(r; -\eta) \quad (1)$$

where $P(r; \eta)$ is the pair connectedness function at some radial distance r and reduced density η for the continuum percolation models and $h(r; \eta)$ is the total correlation function for the equilibrium hard-particle models.² It was shown that the large- d percolation threshold η_c of overlapping hyperspheres and hypercubes is directly related to the large- d freezing-point density of corresponding equilibrium hard-particle models.¹ The extension of these results for overlapping hyperspheres and hypercubes to the case of overlapping particles of general *anisotropic* shape in d dimensions with a specified orientational probability distribution was also described.

The bounds and approximations reported in paper I were applied to assess the accuracy of previous computer simulation results for η_c that span dimensions up to $d = 20$ in the case of overlapping hyperspheres^{3,4} and up to $d = 15$ in the case of hypercubes.⁴ It is convenient to restate the best lower bound on η_c that was found in Ref. 1, namely,

$$\eta_c \geq \frac{1 + \frac{C_3}{2^{2d}}}{2^d \left[1 + \frac{2C_3}{2^{2d}} + \frac{C_4}{2^{3d}} \right]}, \quad (2)$$

where C_3 and C_4 are the trimer and tetramer statistics defined and computed as a function of d in paper I. Comparison of this lower bound to Krüger’s simulation data for hyperspheres revealed that the bound became progressively tighter as d increased and became an excellent estimate for $d \geq 7$. Since it becomes increasingly challenging to estimate percolation thresholds from simulations in high dimensions, it was not surprising that even Krüger’s high-quality simulation data fell slightly below the lower bound (2) for $8 \leq d \leq 11$. The analytical results of paper I revealed that the simulation data reported in Ref. 4 for both hyperspheres and hypercubes were considerably more problematic. In particular, the authors reported incorrectly that the quantity $2^d \eta_c$ for these systems were nonmonotonic in dimension and that hyperspheres have lower thresholds than hypercubes in higher dimensions while the reverse is true in lower dimensions.

One of the main purposes of the present paper is to exploit the accuracy of the lower bound (2) to provide an efficient simulation method, called the *rescaled-particle* algorithm, to estimate continuum percolation thresholds across many dimensions. Another objective is to obtain an upper bound on η_c as well as to provide additional analytical results for certain cluster statistics. In Sec. II, we derive these analytical results. In Sec. III, we describe in detail the rescaled-particle method, which is applicable for general continuum percolation models (e.g., spherical and nonspherical particle shapes). Results for the thresholds of both overlapping hyperspheres and oriented hypercubes for $3 \leq d \leq 11$ are compared to upper and lower bounds on η_c in Sec. IV. In Sec. V, we summarize our conclusions and discuss future work.

II. ADDITIONAL ANALYTICAL RESULTS

A. Basic Definitions

A prototypical continuum percolation model consists of equal-sized overlapping (Poisson distributed) hyperparticles in \mathbb{R}^d at number density ρ ; see paper I and numerous references therein. It is convenient to introduce the reduced number density η , defined by the relation

$$\eta = \rho v_1, \tag{3}$$

where v_1 is the d -dimensional volume of a hyperparticle; see Ref. 1 for an explicit expression of this quantity for a hypersphere, for example. A cluster statistic that has been considered

by various investigators in one, two and three dimensions for overlapping spheres is n_k , the average number of k -mers per unit number of particles.^{5–8} This k -mer statistic obeys the following constraint

$$\sum_{k=1} kn_k = 1, \quad (4)$$

where it is to be noted that $p_k \equiv kn_k$ is the probability that a given particle is part of a k -mer.⁸ In what follows, we will derive estimates for n_k and related cluster statistics for arbitrary dimension.

It was shown in Ref. 8 that n_k can be explicitly expressed for any d for overlapping hyperspheres as certain multidimensional integrals involving exponentials whose arguments contain the union volume of k “exclusion spheres.” Two spheres of radius $D/2$ are considered to be connected if they overlap, i.e., if the center of one lies within a spherical “exclusion” region of radius D centered around the other sphere (see Fig. 3 of paper I). For example, for $k = 1$, $k = 2$ and $k = 3$, we have

$$n_1 = \exp[-2^d \eta] \quad (5)$$

$$n_2 = \frac{\rho}{2} \int_{\mathbb{R}^d} \exp[-\rho v_2(r; D)] f(r) d\mathbf{r} \quad (6)$$

$$n_3 = \frac{\rho^2}{6} \int_{\mathbb{R}^d} d\mathbf{r}_{12} \int_{\mathbb{R}^d} d\mathbf{r}_{13} f(r_{12}) f(r_{23}) \exp[-\rho v_3(r_{12}, r_{13}, r_{23}; D)] \\ + \frac{\rho^2}{3} \int_{\mathbb{R}^d} d\mathbf{r}_{12} \int_{\mathbb{R}^d} d\mathbf{r}_{13} \exp[-\rho v_3(r_{12}, r_{13}, r_{23}; D)], \quad (7)$$

where $v_n(\mathbf{r}_1, \mathbf{r}_2, \dots, \mathbf{r}_n; D)$ is the union volume of n spheres of radius D centered at positions $\mathbf{r}_1, \mathbf{r}_2, \dots, \mathbf{r}_n$, $\mathbf{r}_{ij} = \mathbf{r}_j - \mathbf{r}_i$ and $r_{ij} = |\mathbf{r}_{ij}|$ ($i \neq j$). Moreover, the radial function $f(r)$ defines the connectedness criterion, i.e.,

$$f(r) = \Theta(D - r), \quad (8)$$

and

$$\Theta(x) = \begin{cases} 1, & x \geq 0, \\ 0, & x < 0 \end{cases} \quad (9)$$

is the Heaviside step function. Note that the factor 2^d , appearing in Eq. (5), is the ratio of the exclusion volume v_{ex} to the volume of a sphere. By virtue of the fact that the spheres are Poisson distributed in space, it follows that the mean number of overlaps per sphere \mathcal{N} is given by

$$\mathcal{N} = \rho v_{ex} = 2^d \eta. \quad (10)$$

The *average number of clusters per unit volume* ρ_c is directly related to the sum over n_k ,⁸ namely

$$\frac{\rho_c}{\rho} = \sum_{k=1}^{\infty} n_k. \quad (11)$$

Note that the ratio ρ_c/ρ is the *average number of clusters per particle* and its derivative with respect to ρ (or η) determines the contact value of the *blocking function* $B(r)$,⁹ which is directly related to the conditional probability of finding two particles belonging to different clusters separated by distance r , given that one of the particles is at the origin. For example, in the case of hyperspheres of diameter D , the three-dimensional expression given in Ref. 9 generalizes as follows:

$$\frac{d(\rho_c/\rho)}{d\eta} = -2^{d-1}B(D). \quad (12)$$

We recall here that for overlapping hyperspheres, the blocking function $B(r)$ can be obtained immediately from the pair connectedness function $P(r)$ for any radial distance r via the relation⁶

$$P(r) + B(r) = 1. \quad (13)$$

The fact that $P(r)$ is bounded in the interval $[0, 1]$, implies the same bounds on $B(r)$.

The *average cluster number* Q is the average number of particles in a randomly chosen cluster and is the inverse of ρ_c/ρ ,⁸ namely,

$$Q = \frac{\rho}{\rho_c} = \left(\sum_{k=1}^{\infty} n_k \right)^{-1}. \quad (14)$$

This is to be distinguished from the cluster number S (average number of particles in the cluster containing a randomly chosen particle), which is related to the second moment of n_k .⁵

$$S = \sum_{k=1}^{\infty} k^2 n_k, \quad \eta < \eta_c. \quad (15)$$

Unlike S , which can also be expressed in terms of the pair connectedness function $P(r)$,¹ the average cluster number Q does not diverge at the percolation threshold when $d \geq 2$.⁸

B. Estimates of Cluster Statistics and Upper Bounds on η_c and \mathcal{N}_c

It was shown in Ref. 1 that the mean number of overlaps per sphere at the threshold \mathcal{N}_c [cf. (10)] tends to unity as $d \rightarrow \infty$, i.e.,

$$\mathcal{N}_c \equiv \eta_c \frac{v_{\text{ex}}}{v_1} \sim 1, \quad d \rightarrow \infty, \quad (16)$$

which applies to spherical as well as nonspherical particles (with specified orientational distribution). This does not mean that the concentrations of monomers, dimers, trimers, etc. at the threshold are negligibly small, even if finite clusters become more ramified as the space dimension grows.¹ To explicitly prove this property, we first observe that the exact formula for n_1 [cf. (5)] together with the exact asymptotic result

$$\eta_c \sim \frac{1}{2^d}, \quad d \rightarrow \infty, \quad (17)$$

which applies to any oriented centrally symmetric particle (e.g., spheres, cubes, ellipsoids, etc.)¹, implies the following asymptotic result

$$n_1 \sim \exp(-1) = 0.3678794 \dots, \quad d \rightarrow \infty. \quad (18)$$

We will now show that as d becomes large, monomers, as opposed to any k -mer for $k \geq 2$, are dominant in so far as concentration is concerned, i.e., n_1 is appreciably larger than n_2 and therefore is appreciably larger than n_k with $k \geq 3$, since $n_k > n_{k+1}$ for any positive but bounded η . Let us begin with the formula (6) for the dimer statistic n_2 , which we can rewrite as follows:

$$n_2 = d2^{d-1}\eta \exp[-2^{d+1}\eta] \int_0^D r^{d-1} \exp[2^d\eta\alpha(r; D)], \quad (19)$$

where

$$\alpha(r; R) = \frac{v_2^{\text{int}}(r; R)}{v_1(R)} = \frac{2\Gamma(1 + d/2)}{\sqrt{\pi}\Gamma((d+1)/2)} \int_0^{\cos^{-1}(r/(2R))} \sin(\theta)^d d\theta \quad (20)$$

Here we have used the fact that $v_2(r; R) = 2v_1(R) - v_2^{\text{int}}(r; R)$, where the latter quantity is the intersection volume of two spheres of radius R whose centers are separated by the distance r . The dimensionless intersection volume $\alpha(r; R)$, which has support in the interval $[0, 2R]$, has been explicitly given for any d in a variety of representations^{1,10} and played an important role in paper I. Now since $\alpha(D; D)$ decays to zero exponentially fast according to

the asymptotic relation¹⁰

$$\alpha(D; D) \sim \left(\frac{6}{\pi}\right)^{1/2} \left(\frac{3}{4}\right)^{d/2} \frac{1}{d^{1/2}}, \quad (21)$$

it immediately follows from (19) and (17) that

$$n_2 \sim \frac{\exp(-2)}{2} = 0.06766764 \dots, \quad d \rightarrow \infty, \quad (22)$$

and hence we find

$$\frac{n_1}{n_2} \sim 2 \exp(1) = 5.436563 \dots, \quad d \rightarrow \infty, \quad (23)$$

which is what we set out to prove.

We now derive lower bounds on n_k for $k \geq 2$ as a function of d for any η . Let us begin with the case $k = 2$. Since $\alpha(r; D)$ is a monotonically decreasing function of r , we have that $\alpha(D; D) \leq \alpha(r; D)$ in the interval $[0, D]$ and hence combined with the exact formula (19) yields the lower bound

$$n_2 \geq 2^{d-1} \eta \exp[-2^{d+1} \eta] \exp[2^d \eta \alpha(D; D)]. \quad (24)$$

It is noteworthy that in light of (21), the lower bound (24) becomes asymptotically exact in the high- d limit, i.e., we recover (22). Using similar arguments and the formulas for n_k given in Ref. 8, we obtain the following generally weaker lower bounds on n_k for any k :

$$n_k \geq \frac{2^{(k-1)d}}{k(k-1)!} \eta^{k-1} \exp[-k 2^d \eta]. \quad (25)$$

While for $k = 1$, this bound is exact, it is weaker than (24) for $k = 2$.

Through second order in η , formulas (5), (6) and (7) for n_1 , n_2 and n_3 , respectively, yield

$$n_1 = 1 - 2^d \eta + 2^{2d-1} \eta^2 + \mathcal{O}(\eta^3) \quad (26)$$

$$n_2 = 2^{d-1} \eta - \left(2^{2d} + \frac{C_3}{2}\right) \eta^2 + \mathcal{O}(\eta^3) \quad (27)$$

$$n_3 = \left(2^{2d-1} + \frac{C_3}{3}\right) \eta^2 + \mathcal{O}(\eta^3) \quad (28)$$

Similarly, using expression (14) and the relations immediately above, we can obtain the corresponding density expansion for Q :

$$Q = 1 + 2^{d-1} \eta + \left(2^{2(d-1)} + \frac{C_3}{6}\right) \eta^2 + \mathcal{O}(\eta^3) \quad (29)$$

It was noted in Ref. 1 that the pole of the $[1,1]$ Padé approximant of the density expansion of Q for $d = 3$ yielded an upper bound on the threshold η_c for overlapping spheres. For general d , the $[1,1]$ Padé approximant for Q for either overlapping hyperspheres or oriented hypercubes is given by

$$Q_{[1,1]} \approx \frac{1 - \frac{C_3}{3 \cdot 2^d} \eta}{1 - \left[2^{d-1} + \frac{C_3}{3 \cdot 2^d}\right] \eta}, \quad (30)$$

where the trimer statistic C_3 for both models is given in Ref. 1. We now observe that the pole of (30) is an upper bound on η_c for overlapping hyperspheres and oriented hypercubes for any $d \geq 3$, i.e.,

$$\eta_c \leq \frac{1}{2^{d-1} \left[1 + \frac{C_3}{6 \cdot 2^{d-1}}\right]}, \quad d \geq 3. \quad (31)$$

Using the same methods described in paper I, it is straightforward to prove that for sufficiently large d and any $\eta < \eta_c$, relation (30) bounds Q from below and hence (31) is a rigorous upper bound on the threshold. This is consistent with the observation (noted in Sec. II A) that the actual function Q does not diverge when the mean cluster number S diverges, i.e., when $\eta \rightarrow \eta_c$. We will show in Sec. IV that the expression (31) bounds the simulation data for the threshold from above for both hyperspheres and hypercubes for $3 \leq d \leq 11$. Moreover, according to Ref. 1, the second term within the brackets of inequality (31) goes to zero exponentially fast in the limit $d \rightarrow \infty$, and hence this bound asymptotically becomes

$$\eta_c \leq \frac{1}{2^d}, \quad d \rightarrow \infty, \quad (32)$$

which is the exact asymptotic result.¹ Since the lower bound (2) also becomes exact in this high- d limit, the bounds (2) and (31) converge to the exact asymptotic value of 2^{-d} .

Finally, we note that combining relation (14) and the approximant (30) gives the following approximation of ρ_c/ρ :

$$\frac{\rho_c}{\rho} \approx \frac{1 - \left[2^{d-1} + \frac{C_3}{3 \cdot 2^d}\right] \eta}{1 - \frac{C_3}{3 \cdot 2^d} \eta}. \quad (33)$$

Substituting (33) into (12) yields the following the approximation for the contact value of the blocking function

$$B(D) = 1 - P(D) \approx \frac{1}{1 - \frac{C_3}{3 \cdot 2^d} \eta}. \quad (34)$$

In the Appendix, we provide plots of $B(D)$ and $P(D)$ versus η for selected dimensions.

III. EFFICIENT ALGORITHM TO COMPUTE η_c ACROSS ALL DIMENSIONS

A. Particle-Addition Method

A commonly employed approach to estimate the percolation threshold η_c for continuum percolation in two and three dimensions is the particle-addition method.^{11–13} Starting from a configuration of a small number of particles with random positions in the simulation domain subject to periodic boundary conditions, new particles are added to the domain sequentially with randomly chosen positions in the simulation domain. Each time a new particle is added, the largest cluster in the system (i.e., the one containing the largest number of particles) is identified using a burning-algorithm.¹⁴ This process is repeated until a system-spanning cluster forms.

Although conceptually intuitive and used across dimensions,^{3,4} this method becomes progressively less computationally efficient as the dimension increases.¹ First, to obtain accurate estimates of the percolation threshold, the size of the particles should be much smaller than the linear extent of simulation domain so that adding a single particle leads to a very small increase in the reduced density η . Without *a priori* knowledge of the percolation threshold, one needs to start with sufficiently dilute particle configurations, i.e., with very small η . Therefore, an extremely large number of particles needs to be added to the simulation domain until the system percolates. For each particle addition, one needs to identify the largest cluster and check whether it spans the system, which makes the method computationally very expensive. Moreover, the dynamic nature of particle addition makes it difficult to implement efficient methods to check for local particle connectivity (overlaps of pairs of particles, e.g., the cell method). This problem increases in severity as the dimension increases.

We note that highly efficient algorithms have been developed for investigating clustering and percolation properties of overlapping disks in two dimensions. For example, several frontier-tracking methods have been devised to provide very precise estimates of the percolation threshold η_c of overlapping disks.^{15–17} However, such algorithms cannot be applied in higher dimensions because there is no analogous localized boundary in the gradient percolation method for high-dimensional systems.¹⁸ Other efficient variations of the particle addition method have been implemented, e.g., particles are added only to a single growing

cluster, and the cluster-size distribution rather than the spanning cluster is used to obtain η_c ,¹⁹ and rapid “union-find” methods have been developed to keep track of the connected clusters as particles are added.²⁰ However, these variations of the particle-addition method, although much more efficient than the original one, becomes progressively more difficult to apply as the dimension increases.

B. Rescaled-Particle Method

Tight rigorous lower bounds on the percolation threshold, such as the ones derived in Ref. 1, enable us to devise a highly efficient method to estimate η_c for overlapping particles with arbitrary shapes and orientations in \mathbb{R}^d . The basic idea is to generate initial static particle configurations at a value of η that is taken to be the best lower-bound value, allowing one to finally arrive at the critical value in a computationally efficient manner, even in high dimensions. We note that procedures in which particles are rescaled to obtain η_c have been previously proposed.²¹ However, to the best of our knowledge, our method is the first one to combine the particle rescaling procedure with the tightest lower bound values to efficiently and accurately obtain η_c .

Initially, a Poisson distribution of a large number of points in the simulation domain is generated. Each point in configuration is then taken to be the centroid of a particle with a specified or random orientation and a characteristic particle length scale ℓ_0 (e.g., the diameter of a sphere). The initial value of ℓ_0 is chosen such that the reduced density η of the system equals the tightest lower bound value. For each particle i , a near-neighbor list (NNL) is obtained that contains the centroids of the particles j whose distance D_{ij} to particle i is smaller than $\gamma\ell_0$ ($\gamma > 1$). The value of γ generally depends on the continuum-percolation models of interest. A rule of thumb for a choosing good value of γ is that the NNL list only contains particles that overlap at the percolation threshold. In our simulation for hyperspheres and hypercubes, we have used $\gamma \in [1.05, 1.5]$, depending on the space dimension. Then the particle sizes are slowly and uniformly increased by increasing ℓ_0 (i.e., rescaling the particles), which leads to an increase of the reduced density by a small amount $\delta\eta$. After each rescaling, the particles in the NNL are checked for overlap and the largest cluster in the system is identified. The process is repeated until a system-spanning cluster forms.

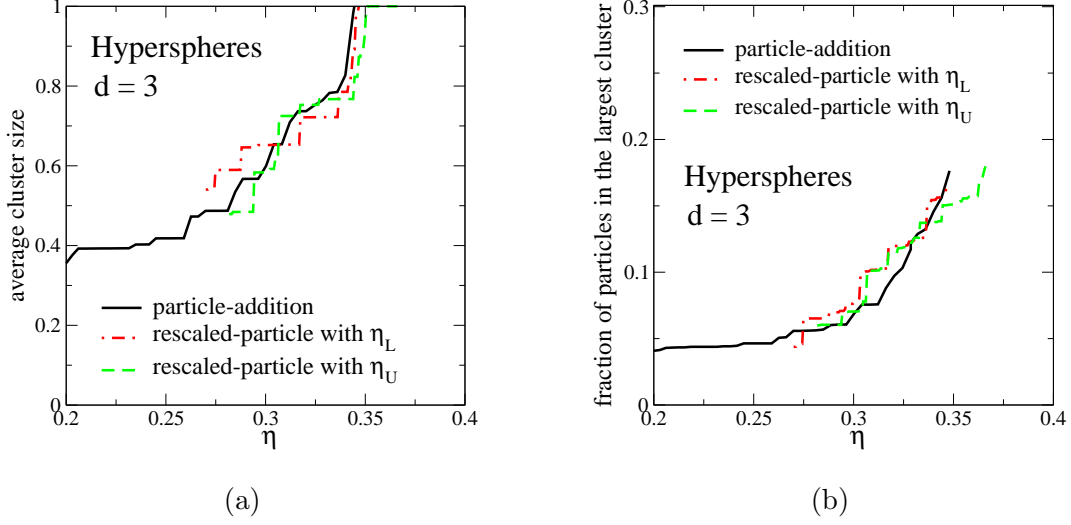


FIG. 1: Cluster statistics, including the linear size of the largest cluster²² (a) and the fraction of particles in the largest cluster (b), associated with the particle-addition and rescaled-particle methods for overlapping hyperspheres in \mathbb{R}^3 . The different methods clearly produce very similar cluster statistics yet the rescaled-particle method is much more computationally efficient, as explained in the text.

Since static particle configurations and predetermined NNL are used, the complexity for identifying clusters is significantly reduced. In addition, as the space dimension increases, it was shown that the lower bounds derived in paper I become increasingly tighter.¹ Thus, total number of rescaling before percolation is achieved is much smaller than the total number of particle additions, which dramatically improves the efficiency of the algorithm. Furthermore, the increase of the reduced density $\delta\eta$ can take arbitrarily small values when η_c is approached, rather than a fixed discontinuous value determined by the particle size via particle-addition methods. This smooth approach to the critical value allows a more accurate estimate of the percolation threshold.

Similarly, given an upper bound on η_c , such as inequality (31), one can start with a percolated system, and rescale the particles (i.e., decreasing the particle size ℓ_0) to reduce η . Figure 1 shows the cluster statistics (e.g., the linear size of the largest cluster²² and the fraction of particles in the largest cluster) associated with the particle-addition method and the rescaled-particle method for overlapping hyperspheres in \mathbb{R}^3 . The initial configurations for the rescaled-particle method include both a non-percolated configuration with η equal to

the lower-bound value η_L and a percolated configuration with η equal to the upper-bound value η_U . We note that close to percolation, the cluster containing the largest number of particles also possesses the largest linear size.

It is clear that the particle-addition method and the rescaled-particle method produce very similar cluster statistics yet the rescaled-particle method is considerably more computationally efficient in three dimensions. The computational efficiency improves for overlapping hyperspheres and hypercubes as the space dimension increases beyond three. Since the upper bound on η_c derived here is not as tight as the lower bound in relatively low dimensions, we mainly use the rescaled-particle method starting from non-percolated configurations with η equal to the tightest lower-bound value, as predicted from (2). However, as noted in Sec. II B, as $d \rightarrow \infty$, both the upper and lower bounds converge to the exact asymptotic value of 2^{-d} .

IV. SIMULATION RESULTS FOR OVERLAPPING HYPERSPHERES AND ORIENTED HYPERCUBES

Using the rescaled-particle method starting from a reduced density given by the lower-bound estimate (2), we compute the percolation threshold for overlapping hyperspheres and oriented hypercubes in dimensions two through eleven. For each dimension, different system sizes N are used. Specifically, we employ $N = 10000, 50000, 100000$ for $d = 2, 3, 4$, $N = 50000, 100000, 500000$ for $d = 5, 6, 7$, $N = 100000, 500000, 1000000$ for $d = 8, 9, 10$, and $N = 1000000, 2500000, 5000000$ for $d = 11$ and the results are extrapolated by spline fitting the finite-system-size data in a log-log plot to obtain the infinite-system-size estimate of η_c . For each system size, the percolation threshold is obtained by averaging over 1000 independent particle configurations for $d = 2$ and 3, 500 independent particle configurations for $4 \leq d \leq 8$, and 100 independent particle configurations for $9 \leq d \leq 11$.

The obtained percolation threshold values η_c for overlapping hyperspheres and hypercubes in dimensions two through eleven are respectively given in Table 1 and Table 2, and displayed in Figs. 2 and 3. We also provide in the tables and figures the corresponding values of the lower bound (2) and upper bound (31) on η_c for purposes of comparison. Note that our simulation data lie very close to the lower-bound values, and that the lower bounds and data converge quickly to one another as d increases. Moreover, we include the numerical

TABLE I: Estimates of the percolation threshold η_c for overlapping hyperspheres as obtained from the rescaled-particle algorithm, the lower bound (2), and the upper bound (31). Also included are the numerical estimates η_c^* of the percolation threshold from a previous study³ that satisfy the bounds (2) and (31). These results are not reported for $d \geq 8$ because they violate the lower bounds.

d	η_c^L	η_c^*	η_c	η_c^U
2	0.748742...	1.1282	1.12810(3)	
3	0.271206...	0.3418	0.34289(2)	0.363636...
4	0.111527...	0.1300	0.1304(5)	0.167373...
5	0.0488542...	0.0543	0.05443(7)	0.0788179...
6	0.0222117...	0.02346	0.02339(5)	0.0376720...
7	0.0103452...	0.0105	0.01051(3)	0.0181921...
8	0.00489917...		0.004904(6)	0.00885075...
9	0.00234800...		0.002353(4)	0.00432995...
10	0.00113534...		0.001138(3)	0.00212726...
11	0.000552682...		0.0005530(3)	0.00104854...

estimates of η_c from previous simulation studies for hyperspheres³ and hypercubes⁴ in case they do not violate the bounds (2) and (31). It can be clearly seen that our rescaled-particle method yields much more accurate estimates of η_c , especially in high dimensions, since we start with particle configurations that are already very close to percolation.

Following Ref. 1, we use the threshold estimate obtained from the $[2, 1]$ Padé approximant of S as the basis to obtain accurate analytical approximations for η_c that applies across all dimensions for hyperspheres and oriented hypercubes. Specifically, we fit the following function to the simulation data for $2 \leq d \leq 11$:

$$\eta_c \approx \left(1 + \frac{b_1}{d^2} + \frac{b_2}{d^4}\right) \eta_0^{(2)}, \quad (35)$$

where

$$\eta_0^{(2)} = \frac{1 + \frac{C_3}{2^{2d}}}{2^d \left[1 + \frac{2C_3}{2^{2d}} + \frac{C_4}{2^{3d}}\right]} \quad (36)$$

TABLE II: Estimates of the percolation threshold η_c for overlapping hypercubes as obtained from the rescaled-particle algorithm, the lower bound (2), and the upper bound (31). Also included are the numerical estimates η_c^* of the percolation threshold from a previous study⁴ that satisfy the bounds (2) and (31). These results are not reported for $d \geq 5$ because they violate the lower bounds.

d	η_c^L	η_c^*	η_c	η_c^U
2	0.732558...	1.098	1.0982(3)	
3	0.256680...	0.3248	0.3247(3)	0.347824...
4	0.103286...	0.12	0.1201(6)	0.158416...
5	0.0447161...		0.05024(7)	0.0742456...
6	0.0202386...		0.02104(8)	0.0354571...
7	0.0094301...		0.01004(5)	0.0171512...
8	0.00448213...		0.004498(5)	0.00837119...
9	0.00216025...		0.002166(4)	0.00411207...
10	0.00105159...		0.001058(4)	0.00202930...
11	0.000515602...		0.0005160(3)	0.00100485...

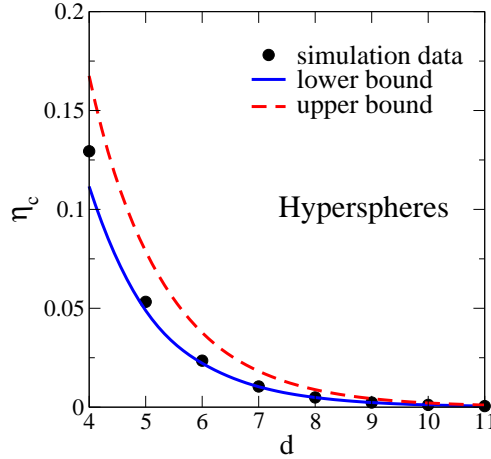


FIG. 2: Percolation threshold η_c versus dimension d for overlapping hyperspheres as obtained from the lower bound (2), the upper bound (31) and the simulation data.

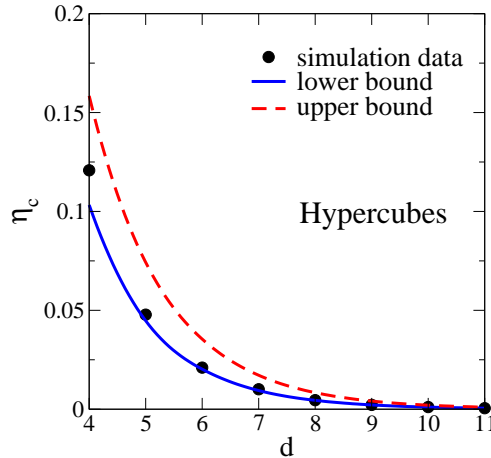


FIG. 3: Percolation threshold η_c versus dimension d for overlapping hypercubes as obtained from the lower bound (2), the upper bound (31) and the simulation data.

is the pole associated with the $[2, 1]$ Padé approximant for the mean cluster number S , i.e., the tightest lower bound for η_c , explicitly given by Eq. (119) of paper I. This lower bound becomes exact for sufficiently large d . Therefore, in agreement with the conclusions of Ref. 1, we see that the high-dimensional percolation behavior is an important contribution to the low-dimensional percolation value. In other words, low-dimensional results encode high-dimensional information.

We find that $b_1 = 2.45074$ and $b_2 = -1.65036$ for hyperspheres with correlation coefficient equal to 0.993194; and $b_1 = 2.57917$ and $b_2 = -2.29755$ for hypercubes with correlation coefficient equal to 0.992262. Note that due to the quality of the available numerical data reported in paper I, the analogous analytical approximations based on those data for hyperspheres and hypercubes only used numerical threshold estimates for $2 \leq d \leq 7$ and $2 \leq d \leq 4$, respectively. Thus, the formula (35) for hyperspheres and hypercubes supersedes in accuracy the ones provided in Ref. 1.

As pointed out in Ref. 1, the numerical estimates of η_c for hypercubes in $5 \leq d \leq 15$ by Wagner *et al.*⁴ violate the tightest lower bound (2). In addition, these simulation data are questionable in high dimensions since the mean number of overlaps per particle \mathcal{N} [defined in Eq. (10)] evaluated at the percolation threshold, i.e., $\mathcal{N}_c = 2^d \eta_c$ is incorrectly found to

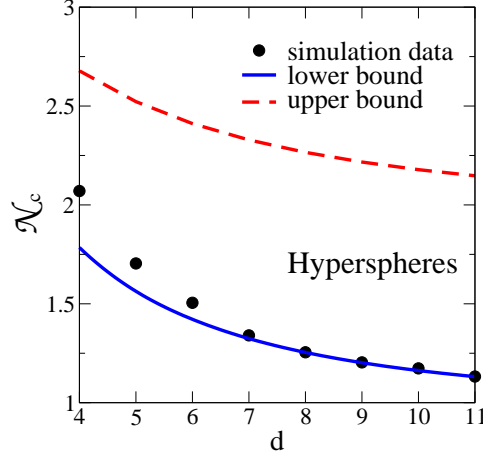


FIG. 4: The mean number of overlaps per hypersphere at percolation threshold $\mathcal{N}_c = 2^d \eta_c$ as a function of d . Also shown are the quantities $2^d \eta_L$ and $2^d \eta_U$, where η_L and η_U are respectively the tightest lower bound (2) and upper bound (31). It is clear that \mathcal{N}_c is a monotonic function of d and quickly converges to the asymptotic value of unity as d increases.

be a nonmonotonic function of d . In particular, these authors found that \mathcal{N}_c first decreases as d increases for $2 \leq d \leq 9$ and then increases as d increases for $10 \leq d \leq 15$. This led to the incorrect conclusion that hyperspheres have lower thresholds than hypercubes in higher dimensions while the reverse is true in lower dimensions.

In Figs. 4 and 5, we show \mathcal{N}_c as a function of d computed using the estimates of η_c obtained from our simulations for overlapping hyperspheres and hypercubes, respectively. The quantities $2^d \eta_L$ and $2^d \eta_U$ are also shown for purposes of comparison, where η_L and η_U are respectively the tightest lower bound (2) and upper bound (31). It can be clearly seen that \mathcal{N}_c for both overlapping hyperspheres and hypercubes are indeed monotonic functions of d , which quickly converge to the asymptotic value of unity as d increases. This indicates again that the large- d asymptotic percolation value is an important contribution to the low-dimensional percolation value. Moreover, one can see from Tables 1 and 2 that hypercubes always have a lower threshold than hyperspheres for any fixed finite dimension, and the thresholds of these two systems approach one another in the limit $d \rightarrow \infty$, as predicted in Ref. 1.

In Fig. 6, we plot the concentration of monomers and dimers, n_1 and n_2 , at the percolation threshold η_c as a function of dimension d for overlapping hyperspheres as obtained from the

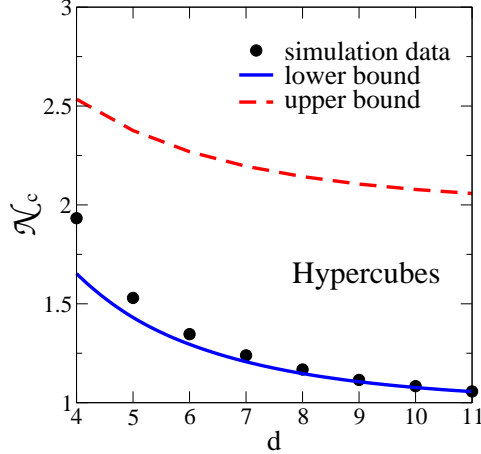


FIG. 5: The mean number of overlaps per hypercube at percolation threshold $\mathcal{N}_c = 2^d \eta_c$ as a function of d . Also shown are the quantities $2^d \eta_L$ and $2^d \eta_U$, where η_L and η_U are respectively the tightest lower bound (2) and upper bound (31). It is clear that \mathcal{N}_c is a monotonic function of d and quickly converges to the asymptotic value of unity as d increases.

exact expressions (5) and (19) and the simulation data for η_c given in Table I. Observe that, consistent with analysis given in Sec. II B, n_1 becomes appreciably larger than n_2 (and hence n_3, n_4 , etc.) as the dimension increases. We include in the figure the lower bound (24) on n_2 , which we see becomes tighter as the space dimension increases, as the analysis of Sec. II B predicts.

V. CONCLUSIONS AND FUTURE WORK

We have supplemented the analytical results obtained in paper I by deriving additional formulas and bounds for certain cluster statistics, such as the concentration of k -mers and related quantities, and obtained an upper bound on the percolation threshold η_c . We utilized this upper bound and the tightest lower bound on η_c obtained in paper I to devise an efficient simulation method, called the *rescaled-particle* algorithm, to estimate continuum percolation properties across many space dimensions. We applied this simulation procedure here to compute, with heretofore unattained accuracy, the threshold η_c and associated mean number of overlaps per particle \mathcal{N}_c for both overlapping hyperspheres and oriented hypercubes for $3 \leq d \leq 11$. Comparison of these simulations results to corresponding upper and lower bounds on these percolation properties revealed that the bounds converge to one another as

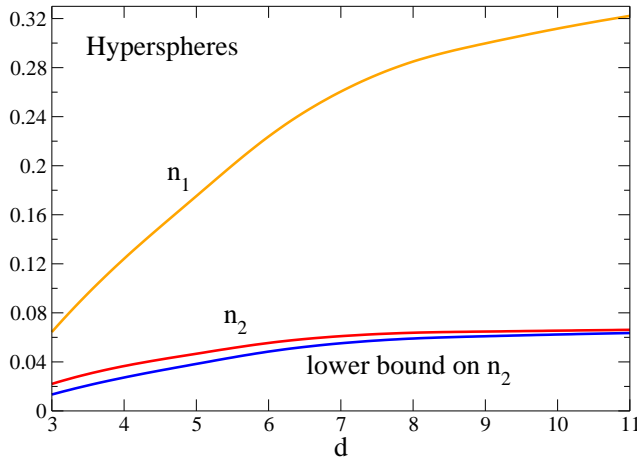


FIG. 6: Monomer and dimer concentrations, n_1 and n_2 , at the percolation threshold η_c as a function of dimension d for overlapping hyperspheres as obtained from the exact expressions (5) and (19) and the simulation data for η_c given in Table I. Included in the figure is the lower bound (24) on n_2 .

the space dimension increases. It is noteworthy that the lower bound provides an excellent estimate of η_c and \mathcal{N}_c , even for relatively low dimensions. We confirmed a prediction of paper I that low-dimensional percolation properties encode high-dimensional information. We also showed that the concentration of monomers dominate over concentration values for higher-order clusters (dimers, trimers, etc.) as the space dimension becomes large. Finally, we provided accurate analytical estimates of the pair connectedness function and blocking function at their contact values for any d as a function of density.

In paper I, the extension of the continuum percolation results obtained for overlapping hyperspheres and oriented hypercubes to cases in which the overlapping hyperparticles are nonspherical (anisotropic in shape) with some specified orientation distribution function (e.g., random orientations) was briefly discussed. Future work will expound on this extension to overlapping anisotropically-shaped hyperparticles with random orientations.. The exploration of the generalizations of the techniques of this series of papers to bound percolation thresholds in the lattice setting¹ (bond and site percolation^{14,23,24}) represents an intriguing area for future research.

Acknowledgements

This work was supported by the Materials Research Science and Engineering Center Program of the National Science Foundation under Grant No. DMR-0820341 and by the Division of Mathematical Sciences at the National Science Foundation under Award Number DMS-1211087.

Appendix: Approximations for the Blocking and Pair Connectedness Functions at Contact

In Sec. II, we noted that the inverse of the cluster number Q is the of the average number of clusters per unit volume ρ_c/ρ [see Eq. (14)]. We derived the approximation (30) for Q , which immediately leads to the approximation (33) for ρ_c/ρ and thus, the approximation (34) for the contact values of the blocking function $B(D)$ and pair connectedness function $P(D)$.

In this appendix, we compare the approximation (33) for ρ_c/ρ versus η with available numerical data for overlapping spheres in \mathbb{R}^3 .⁹ These results are plotted in Fig. 7. Observe that the approximation agrees with the simulation data very well and bounds the data from below.

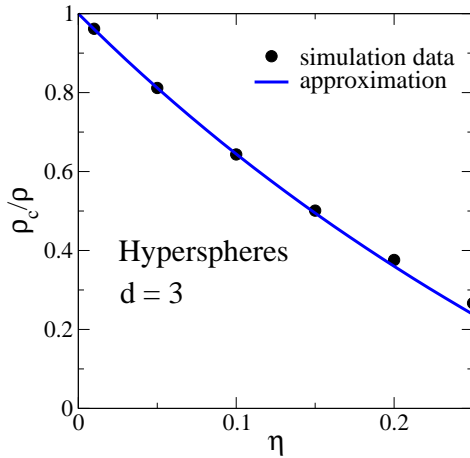


FIG. 7: The approximation (33) of ρ_c/ρ as a function of η for three-dimensional overlapping spheres. Also shown are the simulation data reported in Ref. 9 for purposes of comparison. It can be seen that the approximation agrees very well with the simulation data and bounds the data from below.

Since the approximation (33) for ρ_c/ρ improves as the space dimension increases beyond three, we expect that results derived from it, such as the relation (34) for the blocking function and pair connectedness function at contact, will provide accurate approximations across dimensions for $d \geq 4$. In particular, we provide plots of the contact values $B(D)$ and $P(D) = 1 - B(D)$ [as predicted by (34)] versus η for overlapping hyperspheres in dimensions 3, 7 and 11 up to the respective percolation thresholds in Figs. 8, 9 and 10. The functions $B(D)$ and $P(D)$ are equal to unity and zero, respectively, at $\eta = 0$ and decrease and increase monotonically with increasing η up to η_c . We also see that $B(D)$ and $P(D)$ vary less appreciably with increasing η from the maximum value of unity and minimum value of zero, respectively, as the space dimension increases.

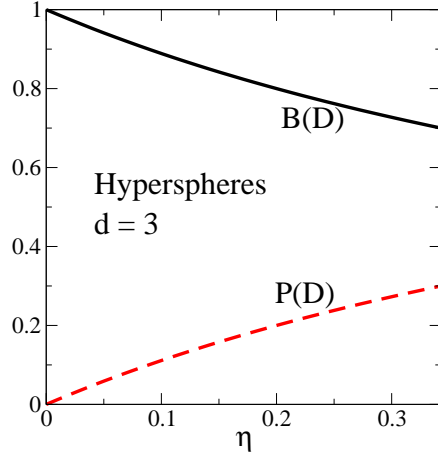


FIG. 8: The contact values of the blocking function $B(D)$ and the pair-connectedness function $P(D)$ versus η up to $\eta_c = 0.34289$ (see Table I) for overlapping spheres in \mathbb{R}^3 . Note that $B(D) + P(D) = 1$ [c.f. (34)].

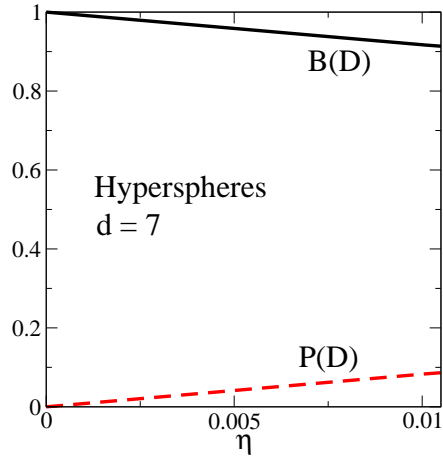


FIG. 9: The contact values of the blocking function $B(D)$ and the pair-connectedness function $P(D)$ versus η up to $\eta_c = 0.01051$ (see Table I) for overlapping hyperspheres in \mathbb{R}^7 . Note that $B(D) + P(D) = 1$ [c.f. (34)].

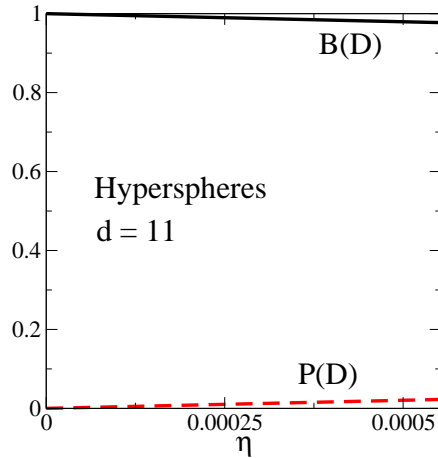


FIG. 10: The contact values of the blocking function $B(D)$ and the pair-connectedness function $P(D)$ versus η up to $\eta_c = 0.0005530$ (see Table I) for overlapping hyperspheres in \mathbb{R}^{11} . Note that $B(D) + P(D) = 1$ [c.f. (34)].

* Electronic address: torquato@electron.princeton.edu

† Electronic address: yjiao@princeton.edu

¹ S. Torquato, J. Chem. Phys. **136**, 054106 (2012).

² For equilibrium hard-particle systems, the total correlation function $h(r; \eta)$ generally takes on both negative and positive values depending on the values of the radial distance r and reduced density η . One can think of the duality relation (1) as the mapping that is required to convert a correlation function for a hard-particle system to a non-negative pair connectedness function (bounded from above by unity) for the corresponding overlapping particle system.

³ A. Krüger, Ph.D. thesis, University of Bielefeld, Germany, 2003.

⁴ N. Wagner, I. Balberg, and D. Klein, Phys. Rev. E **74**, 011127 (2006).

⁵ S. W. Haan and R. Zwanzig, J. Phys. A: Math. Gen. **10**, 1547 (1977).

⁶ A. Coniglio, U. De Angelis, and A. Forlani, J. Phys. A **10**, 1123 (1977).

⁷ A. K. Sen and S. Torquato, J. Chem. Phys. **89**, 3799 (1988).

⁸ J. Quintanilla and S. Torquato, Phys. Rev. E **54**, 5331 (1996).

- ⁹ J. A. Given, I. C. Kim, S. Torquato, and G. Stell, J. Chem. Phys. **93**, 5128 (1990).
- ¹⁰ S. Torquato and F. H. Stillinger, Experimental Math. **15**, 307 (2006).
- ¹¹ M. D. Rintoul and S. Torquato, J. Phys. A: Math. Gen. **30**, L585 (1997).
- ¹² D. R. Baker, G. Paul, S. Sreenivasan, and H. E. Stanley, Phys. Rev. E **66**, 046136 (2002).
- ¹³ Y. B. Yi, C. W. Wang, and A. M. Sastry, J. Electrochem. Soc. **151**, A1292 (2004).
- ¹⁴ D. Stauffer and A. Aharony, *Introduction to Percolation Theory* (Taylor and Francis, London, 1994).
- ¹⁵ J. Quintanilla and S. Torquato, J. Chem. Phys. **111**, 5947 (1999).
- ¹⁶ J. Quintanilla, S. Torquato, and R. M. Ziff, J. Phys. A: Math. & Gen. **33**, L399 (2000).
- ¹⁷ J. A. Quintanilla and R. M. Ziff, Phys. Rev. E **76**, 051115 (2007).
- ¹⁸ J. F. Gouyet, M. Rosso and B. Sapoval, Phys. Rev. B **37**, 1832 (1988).
- ¹⁹ C. D. Lorenz and R. M. Ziff, J. Chem. Phys. **114**, 3659 (2001).
- ²⁰ M. E. Newman and R. M. Ziff, Phys. Rev. E **64**, 016706 (2001).
- ²¹ T. Visek and J. Kertész, J. Phys. A **14**, L31 (1981).
- ²² The linear size of a cluster in \mathbb{R}^d is defined to be the largest distance along any of the d orthogonal directions between the centroids of any pair of particles in the cluster.
- ²³ S. Torquato, *Random Heterogeneous Materials: Microstructure and Macroscopic Properties* (Springer-Verlag, New York, 2002).
- ²⁴ M. Sahimi, *Applications of Percolation Theory* (Taylor and Francis, London, 1994).